Marine Pollution Bulletin 149 (2019) 110496

Contents lists available at ScienceDirect

Marine Pollution Bulletin

journal homepage: www.elsevier.com/locate/marpolbul

Distribution and origination of zinc contamination in newly reclaimed heterogeneous dredger fills: Field investigation and numerical simulation

Linbo Wu[a], Jianxiu Wang[a,b,c,e,*], Xiangjun Pei[c,**], Graham E. Fogg[d], Tianliang Yang[e,f], Xuexin Yan[e,f], Xinlei Huang[e,f], Zipeng Liu[g], Rui Qi[a]

[a] College of Civil Engineering, Tongji University, Shanghai 200092, China
[b] Key Laboratory of Geotechnical and Underground Engineering of Ministry of Education, Tongji University, Shanghai 200092, China
[c] State Key Laboratory of Geohazard Prevention and Geo-environmental Protection, Chengdu University of Technology, Chengdu 610059, China
[d] Department of Land, Air and Water Resources, University of California, Davis 95616, US
[e] Key Laboratory of Land Subsidence Monitoring and Prevention, Ministry of Land and Resources, Shanghai 201204, China
[f] Shanghai Institute of Geological Survey, Shanghai 200072, China
[g] College of Environmental Science and Engineering, Tongji University, Shanghai 200092, China

ARTICLE INFO

Keywords:
Land reclamation
Heterogeneous dredger fills
Zn contamination
Field investigation
Stochastic modeling
Numerical simulation

ABSTRACT

Heavy metal elements, including Zn, Cd, As, Ni, Cu, Pb and Cr, were detected in soils (no deeper than 75 m) from newly reclaimed zones of Shanghai, China. The Zn concentration exceeded soil quality limits. The Zn contamination was tested in both dredger fills and sedimentary layers (①$_{3-3}$, ②$_3$, ④ and ⑤$_{1-1}$). However, it was not detected in layer ⑤$_{1-2}$–⑨. PCA and HCA analysis show that exogenous Zn probably was the contaminant source of dredger fills before the fills were dredged from the neighboring waters. Stochastic heterogeneity of the dredger fills affects the Zn-depollution remarkably. Numerical simulations show both acid precipitation and widespread drainage channels in the zones contributed to Zn-decrease in the dredger fills no deeper than 1.2 m. Acid rainstorms work better than acid constant precipitation in Zn-remediation for layers below 0.4 m. To remove Zn contamination in deep dredger fills, un-consolidation of the fills should be utilized.

1. Introduction

The coastal regions within 60 km from the sea supported almost 60% population in 2016, and the ratio becomes higher in coming years (UN Atlas, 2019). This trend globally results in large-scale development of land reclamation to meet the demand for land. Area of reclaimed land in many countries, such as United States, South Korea and Netherlands exceeds 1000 km^2, China reclaimed the largest area of coastal land (Martín-Antón et al., 2016), over 1860 km^2 lands were reclaimed in China during 2000–2016, and a large portion of the lands hold worrying contamination risk (Wang et al., 2018). Environmental impacts by land reclamation were mainly focused on neighboring water and sediment quality (Manap and Voulvoulis, 2016), biological existence (Erftemeijer et al., 2012; Mostafa, 2012). Actually, contamination including heavy metal contamination within marine sediments and dredged materials was globally detected in many regions (Ho et al., 2002), especially in river estuaries (Caeiro et al., 2005; EPA, 2016; Mukesh et al., 2018). Many land reclamation programs using sediments of unknown quality for fills were conducted under poor environmental supervision especially in developing regions, this means environmental quality of the new lands should also catch enough attention.

Over 300 km^2 land was reclaimed for further development of the city of Shanghai, China (Wang et al., 2014), and large-scale new land reclamation are under construction. Shallow hydraulic dredger fills (at a depth of 0.5–1 m) were detected in 2016 showing no significant contamination in Shanghai's newly reclaimed land, but surface sediments in some Shanghai's coastal zones were detected to be contaminated by Zn (Liu et al., 2000), Cd (Zhang et al., 2009; Fang et al., 2013; Li et al., 2013), As (Li et al., 2013). This implies hydraulic dredger fills in this region were probably contaminated.

Soil structure of hydraulic dredger fills are decided by the fill source (EPA, 1989), complex sedimentary layer faces in river estuaries result in heterogeneity of dredger fills using sediments from neighboring waters. Borehole data showed that explicit heterogeneity of hydraulic reclaimed soils in east Shanghai, and Wang et al. (2019) has established a comprehensive geo-model for a typical reclaimed field in Hengsha

* Correspondence to: J. Wang, Department of Geotechnical Engineering, Tongji University, Shanghai 200092, China.
** Corresponding author.
E-mail addresses: wang_jianxiu@163.com (J. Wang), peixj0119@tom.com (X. Pei).

https://doi.org/10.1016/j.marpolbul.2019.110496
Received 28 March 2019; Received in revised form 5 August 2019; Accepted 6 August 2019
Available online 16 August 2019

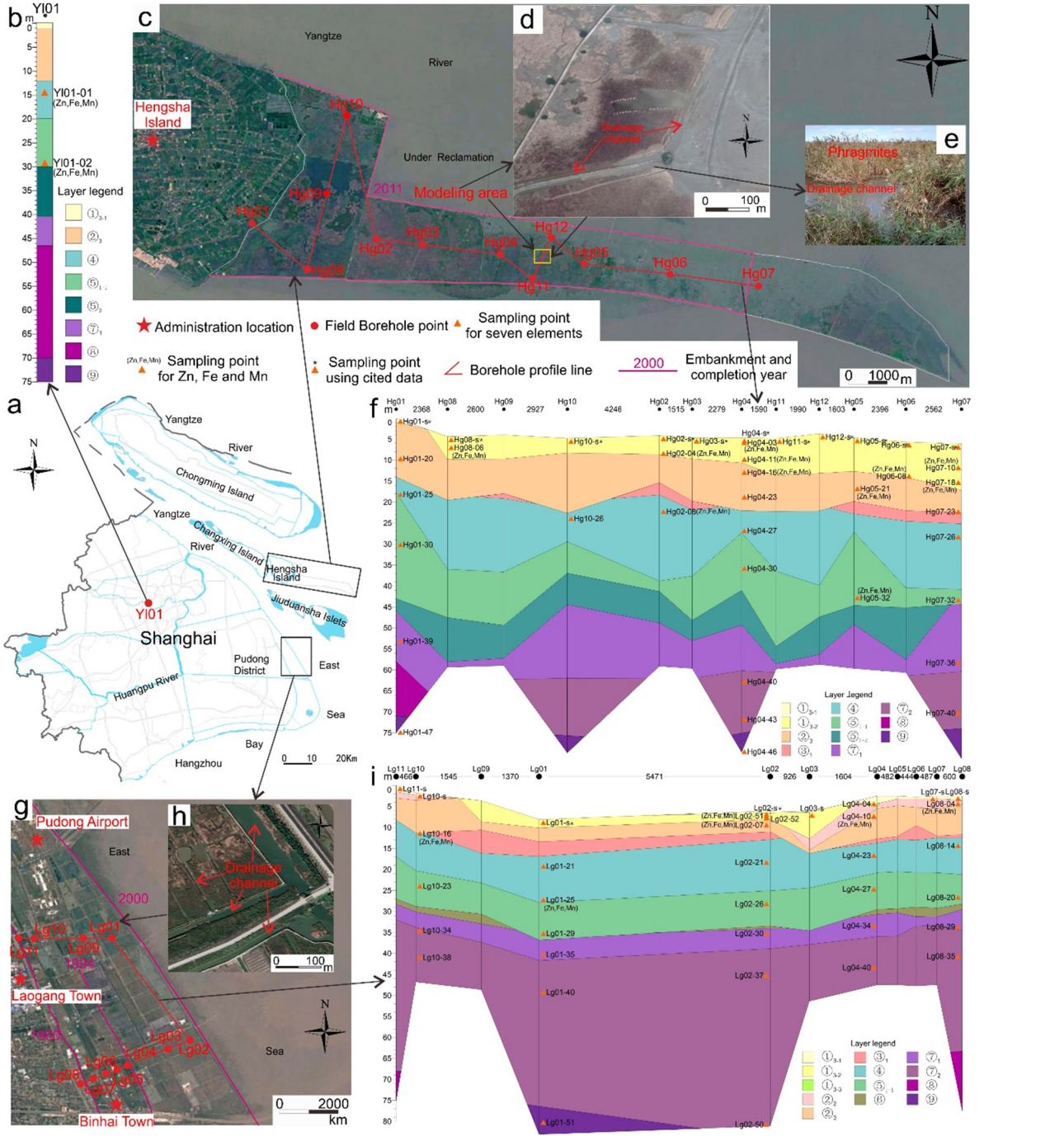

Fig. 1. Geotechnical and topographic background of study zones in Shanghai, China. (a) Geographical map of Shanghai. (b) Strata profile in borehole Yl01 from Yunling zone and samples from there; (c) Satellite image of Hengsha Island photoed in December 2016 and surveyed points there; (d) Satellite image of the numerical modeling zone in Hengsha Island photoed in February 2016; (e) Drainage channel and phragmites in the numerical modeling zone photoed in December 2016; (f) Strata profile in Hengsha Island and samples from there; (g) Satellite image of Laogang Town photoed in December 2016 and surveyed points there; (h) Drainage channels in Laogang Town photoed in October 2018; (f) Strata profile in Laogang Town and samples from there.
(The satellite maps were downloaded from http://www.google.cn/maps)

Island. In this geo-model, heterogeneity of newly reclaimed soils was characterized using stochastic geo-modeling but dredger fills in numerical modeling studies usually were considered as homogeneous layer (Stark et al., 2005; Sun et al., 2015). Numbers of numerical modeling studies were conducted on soil contaminant transport (Bekhit and Hassan, 2005; Appelo and Rolle, 2010), soil contamination remediation (Nützmann et al., 2005), soil contaminant leaching (Kedziorek et al., 1998; Mallants et al., 2011), stochastic geo-modeling (Carle and Fogg, 1997; Nezhad et al., 2011), and these aspects are needed to be integrated into one geo-model to analyze the evolution of solute transport within the heterogeneous newly reclaimed zone since the land was formed. Considering the potential problems caused by the newly reclaimed land in Shanghai, the authors surveyed seven heavy metal contaminations (Zn, Cd, As, Ni, Cu, Pb and Cr) within deep layers (deeper than 1 m) in those land on basis of primary investigation in shallow layers therein. To further explore source of Zn in the soils, concentrations of Zn, Mn and Fe were detected in 20 deep soil samples. Correlations among those elements and correlated factors such as

Table 1
Strata in the study regions.

Strata	Soil type	Strata	Soil type
①$_{3-1}$	Landfill	⑤$_{1-2}$	Silt interbedded with clay
①$_{3-2}$	Dredger fill	⑤$_{3}$	Silty clay
①$_{3-3}$	Disturbed mud	⑥	Silty clay
②$_{2}$	Muddy and silty clay	⑦$_{1}$	Sandy silt
②$_{3}$	Silt	⑦$_{2}$	Silt and sand
③$_{1}$	Muddy and silty clay	⑧	Clay
④	Muddy clay	⑨	Sand with silt
⑤$_{1-1}$	Clay		

depth, soil type were analyzed. Considering the detected contamination distribution, a typical hydraulic reclaimed field was chosen as object for finite difference numerical modeling to explore contaminate transport within the layers.

2. Methods and materials

2.1. Field investigation

Contamination survey and sampling were performed in typical reclaimed fields in Hengsha Island and Laogang Town in 2016 and 2017. Deep sediments were also sampled from Yunling zone, inland Shanghai for comparison in 2017 (Fig. 1). The drilling and sampling depth of all the boreholes were set < 75 m. The surveyed strata are shown in Fig. 1 and Table 1. Twenty nine soil and sediment samples were obtained from twelve boreholes in Hengsha Island (Fig. 1c, f). Thirty five soil samples were obtained from eleven boreholes in Laogang Town (Fig. 1g, i). Two soil samples were obtained from one borehole in Yunling zone (Fig. 1b). The samples were selected in the contamination detection and evaluation. Additionally, eleven surface soil samples from Hengsha Island and two surface samples from Laogang Town detected by Wang et al. (2018) were also included in this work (Fig. 1).

2.2. Laboratory tests

All samples were air-dried and homogenized after removing large debris for element concentration detection. Approximate 0.1 g soil from each sample was taken for the tests. All the tests were done in November 2016. The test methods and other information are shown in Table 2. Duplicates were determined to ensure data quality. The heavy metal concentration data by Wang et al. (2018) were detected together with the 46 soil samples in December 2016. The detected heavy metals can be verified whether exceeding the Environmental Quality Standards for Soil (CEPB and CTSB, 1995) (Table 3). According to the Standards, soil quality of level I aims to keep nature ecosystem background quality, level II to ensure humans' good health, level III to enable both normal operation of agriculture and normal growth of plants, thus the level II and III were the focuses herein. The pH of phreatic water ranged from 7.7 to 8.2 in the surveyed zones (Wang et al., 2018), thus thresholds for pH higher than 6.5 (Table 3) were used to evaluate the soil quality.

2.3. Correlation analysis

Principal component analysis (PCA) was conducted on Zn, Mn and Fe concentrations from 20 soil specimens to examine the source of the Zn within the soils. The 20 specimens were all sampled at the depth no deeper than 39.15 m (⑤$_{1-1}$). In the PCA analysis, varimax rotation (Gotelli and Ellison, 2004) was applied to maximize the sum of the variance of the factor coefficients. Hierarchical clustering analysis (HCA) was performed on the heavy metal contents to explore the correlation among the Zn, Cd, As, Ni, Cu, Pb and Cr in 42 sedimentary samples from the reclaimed zones and their neighboring old intertidal flats. The specimens were all sampled from neighboring zones within

Table 2
Test methods and information of the heavy metal concentration detection.

Sample	Test content	Apparatus	Type	Test time	Test lab
46 soil samples and 1 reagent blanks	Microwave digestion with an HCl-HNO_3-HF mixture	Microwave digest system	Anton Paar Multiwave 3000	Dec., 2016	Instrumental Analysis Center of SJTU
46 soil samples and 1 reagent blank	Concentration of Pb, Zn, Ni, Cu, Cr, Cd, and As	Inductively coupled plasma optical emission spectrometer	Agilent 720ES	Dec., 2016	State Key Laboratory of Pollution Control and Resource Reuse of Tongji University
11 soil samples and 1 reagent blank	Hot plate digestion with an HCl-HNO_3-HF mixture	Digital stainless steel heating plate	Anton Paar Multiwave 3000	Jan., 2018	Instrumental Analysis Center of SJTU
11 soil samples and 1 reagent blank	Concentration of Zn,Fe,Mn	Inductively coupled plasma optical emission spectrometer	Agilent 720ES	Jan., 2018	Instrumental Analysis Center of SJTU
8 soil samples and 1 reagent blank	Hot plate digestion with an HCl-HNO_3-HF mixture	Digital stainless steel heating plate	Guohua DB-4	Feb., 2018	State Key Laboratory of Pollution Control and Resource Reuse of Tongji University
8 soil samples and 1 reagent blank	Concentration of Zn,Fe,Mn	Inductively coupled plasma optical emission spectrometer	iCAP 6300	Feb., 2018	State Key Laboratory of Pollution Control and Resource Reuse of Tongji University

Table 3
Environmental quality standards for soil in China (CEPB and CTSB, 1995).

Level	I	II			III
Background	Nature state	pH < 6.5	6.5 ≤ pH ≤ 7.5	pH > 7.5	pH > 6.5
Cu (ppm)	35	50	100	100	400
Pb (ppm)	35	80	80	80	500
Zn (ppm)	100	200	250	300	500
Cd (ppm)	0.2	0.3	0.3	0.6	1.0
Cr (ppm)	90	250	300	350	300
As (ppm)	15	40	30	25	30
Ni (ppm)	40	40	50	60	200

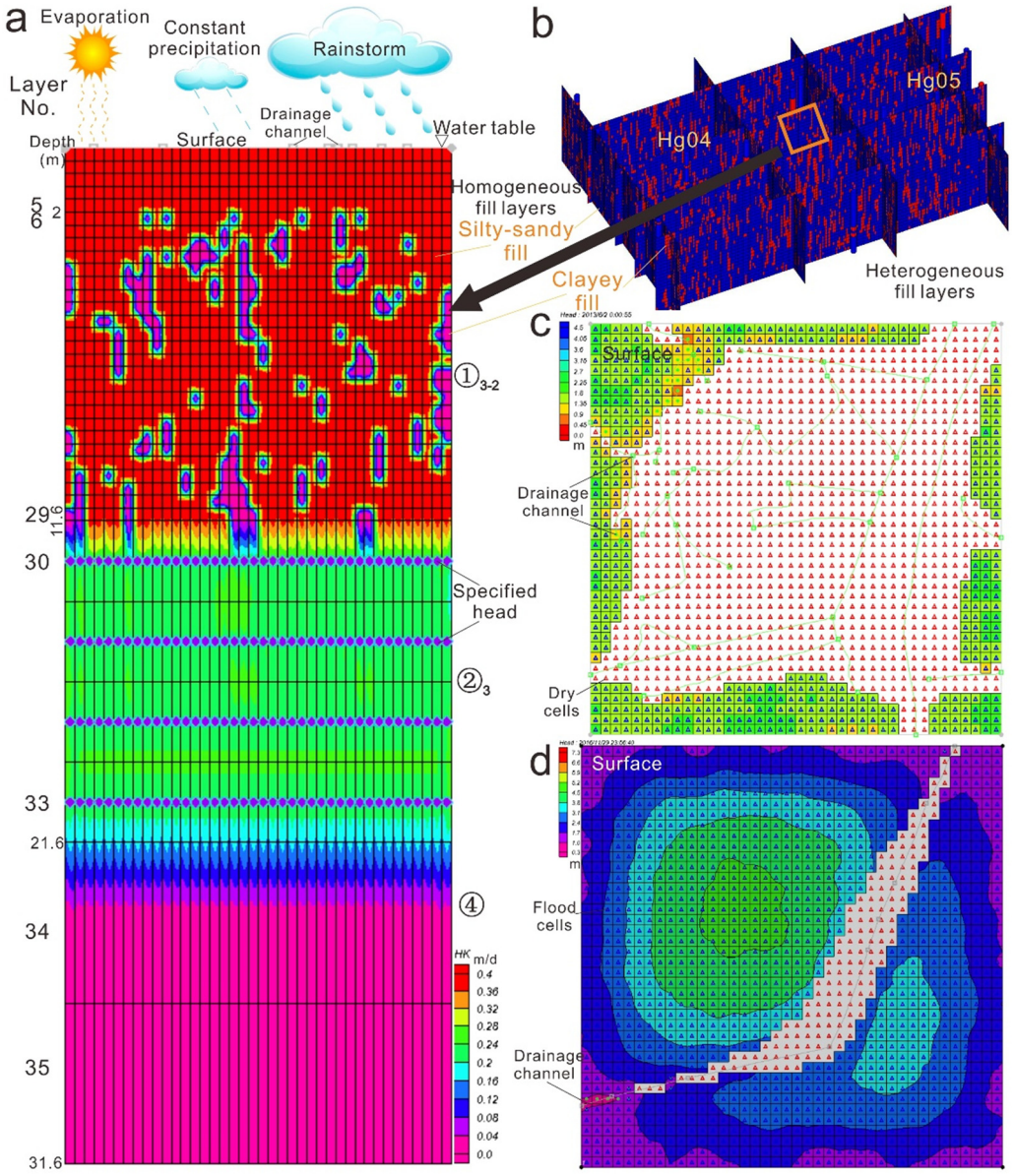

Fig. 2. Geo-model for the numerical analysis. a. K_h contour profile of comprehensive geo-model for the Zn transport modeling; b. Stochastic model for the heterogeneous reclaimed layers; c. Water head contour distribution in the surface layer after one year considering all the drainage channels; d. Water head contour distribution in the surface layer after over four year considering only one typical drainage channel.

Yangtze River estuary, indicating their mineral sources were similar. In the HCA analysis, the squared Euclidean distance linkage method (between-group linkage) was utilized as the basis of the distance metrics, and Z scores were applied to standardize the variable data.

2.4. Numerical model to simulate the evolution of Zn contamination

To understand the present distribution of Zn in shallow and deep soils, numerical model was introduced to simulate the potential transport mechanism of Zn under certain conditions. On basis of the field

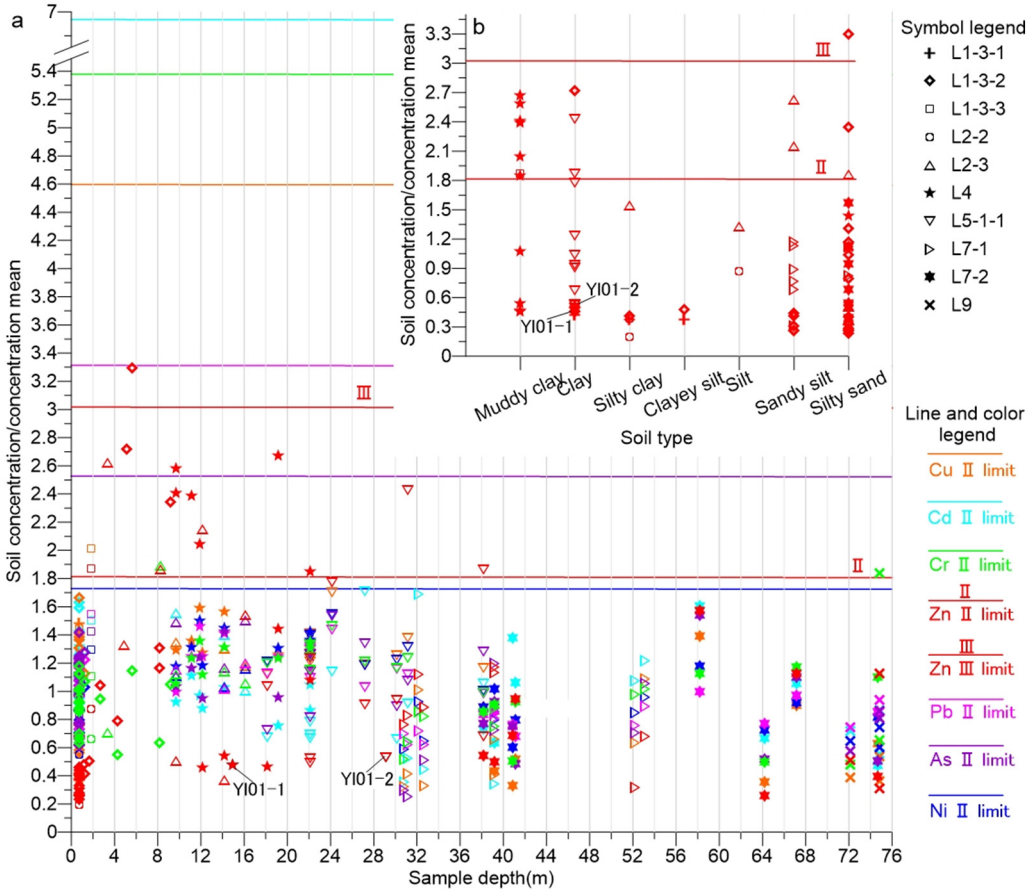

Fig. 3. Distribution of Zn, Cd, As, Ni, Cu, Pb and Cr within the surveyed layers. a. Seven heavy metal element concentration – sample depth – layer information scatter diagram; b Zn concentration – soil type − layer information scatter diagram.

investigation and heavy metal contamination detection, a typical newly reclaimed field in Hengsha Island was chosen for the numerical modeling (Fig. 1c). The selected field contains enough boreholes to ensure validity of the geo-model, and explicit Zn contamination was detected to exist in both the dredger fills and sedimentary layers therein.

2.4.1. Comprehensive geo-model

Considering comprehensively void ratio, compression modulus, horizontal hydraulic conductivity, vertical hydraulic conductivity and density, HCA analysis on different dredger fill types was done to simplify dredger fill types set in the geo-mode. Transitional probability geo-statistics (Carle, 1999) was applied to build a comprehensive geo-model including a stochastic dredger fill geo-model in Hengsha Island (Wang et al., 2019) (Fig. 2a). The comprehensive geo-model was introduced herein. The geo-model consisted of the upper homogeneous fill layers ($①_{3-2}$, layer 1–5), heterogeneous fill layers ($①_{3-2}$, layer 6–29) and layer $②_3$ (Layer 30–33). All the 29 fill layers are 0.4 m thick per single layer (Fig. 2a–b), the $②_3$ is composed of four layers of 2.5 m thick silty-sandy sediments (Fig. 2a). To explore long term influence on the deep clay layer, 10 m layer ④ divided into two equal thick layers (Layer 34–35) were added to the geo-model (Fig. 2a). Depth of phreatic water table in the study zone ranged from 0 m to 0.5 m in December 2016, and soils in the field were saturated when it was reclaimed, thus the groundwater table in the numerical mode was set as 1 m, the same with elevation of the surface (Fig. 2a).

2.4.2. Environmental factors in the numerical model

Given that transport of Zn is sensitive to change of solution pH, and that pH mean of Shanghai's precipitation in 2012–2016 was 4.64 (SMBEE, 2013), 4.81 (SMBEE, 2014), 4.90 (SMBEE, 2015), 5.07 (SMBEE, 2016a), 5.22 (SMBEE, 2017) successively, acid precipitation was assumed as a major reason driving Zn to transport in the weakly alkali environment (Fig. 2a). Total precipitation mean of Shanghai during recent 107 years was 1158.9 mm per year, the subtropical monsoon climate in Shanghai brings 75.2% of the total precipitation in flood season during May to October, and a large portion of its precipitation done as rainstorms. Rainstorm with precipitation over 81 mm/h during 2001–2007 evenly happened twice every year (Lu et al., 2010), thus precipitation occurred in its flood season was divided into two rainstorms per year in the numerical model, and the remaining precipitation happened in constant rate. Rainstorms in Shanghai usually last for several hours, and the surface water brought by rainstorms usually take two to four days to be used up, thus precipitation infiltration by every rainstorm in the numerical modeling lasts for three days. When rainfall intensity becomes larger than soil infiltration capacity, the rainfall infiltration rate should take soil infiltration capacity value, thus 0.048 m/d (Morbidelli et al., 2018) was taken as the infiltration rate during the rainstorms in the numerical modeling. The subtropical monsoon climate in Hengsha Island governing the modeled zone also results in a phreatic evaporation intensity of 547.5 mm/y therein (Yang et al., 2004), which probably affects the phreatic water system remarkably, thus evaporation happened in the modeled zone was also considered in the numerical analysis.

Given that water pH from Huangpu River estuary to the modeling site changes from 7.25 to 8 (Sun et al., 2017), and that solubility of Zn $(OH)_2$ was very low under room temperature and alkali environment (Reichle et al., 1975), thus major formulation of Zn contamination within the modeling site was set as $Zn(OH)_2(c)$. Thus key chemical reactions happened during the modeling should be (Prommer and Post, 2010):

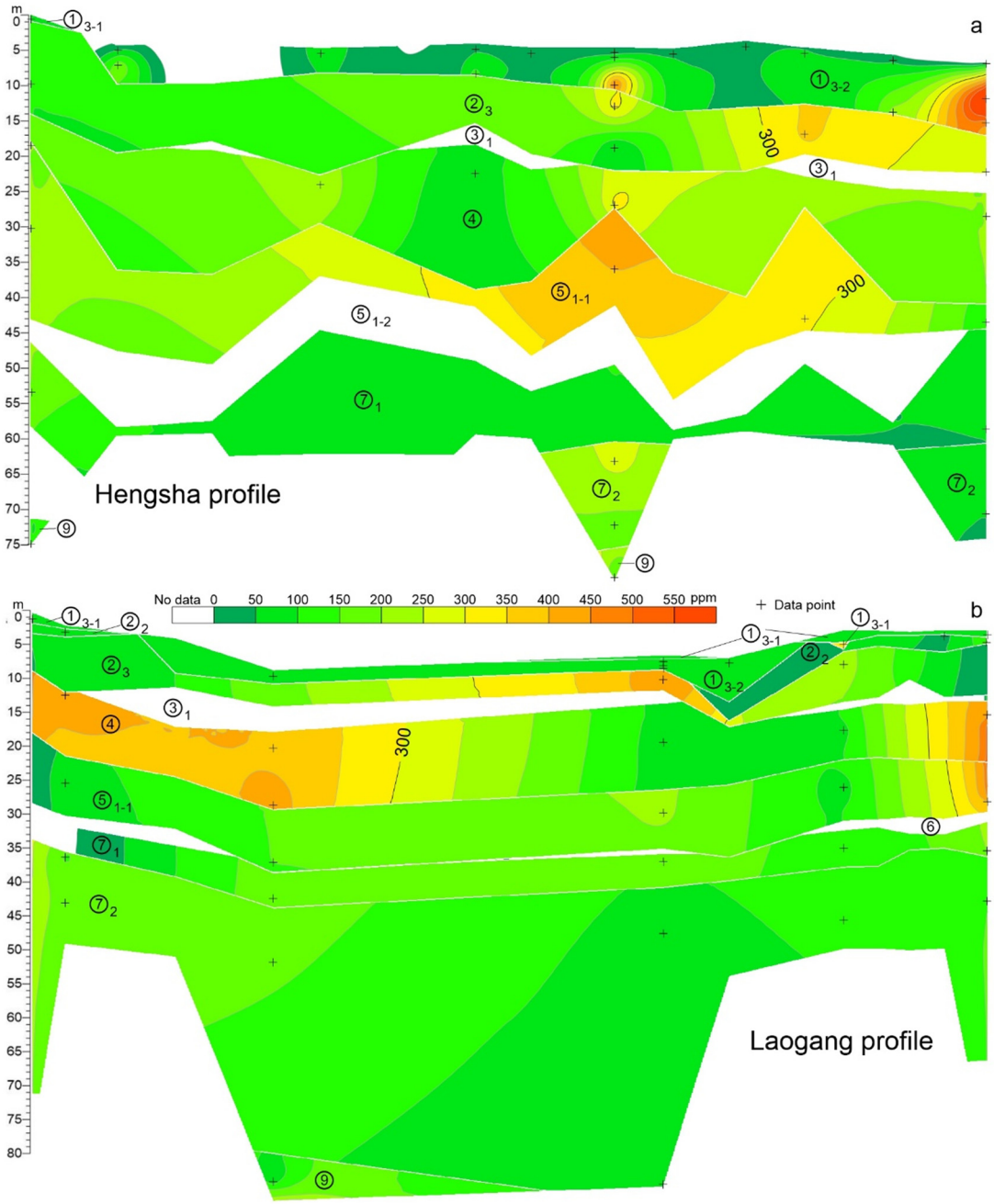

Fig. 4. Zn concentration contour profile using minimum curvature interpolation within depth of 0–75 m. The two profiles share the same legends.

Table 4
Total variance explanation and rotated component matrix (two principal components selected) for Zn, Mn, Fe contents within soils of the surveyed zones. The bold data in the table are the considered data of remarkable analysis significance.

Component	Initial eigenvalues			Heavy metals	Component	
	Total	% of variance	Cumulative %		PC1	PC2
1	**2.015**	**67.161**	**67.161**	Zn	0.109	**0.994**
2	**0.913**	**30.426**	**97.587**	Fe	**0.980**	0.061
3	0.072	2.413	100.000	Mn	**0.969**	0.158

$$OH^- + H^+ \rightleftharpoons H_2O \quad \log k = -14.0 \tag{1}$$

$$Zn^{2+} + H_2O \rightleftharpoons Zn(OH)^+ + H^+ \log k = -8.96 \tag{2}$$

$$Zn^{2+} + 3H_2O \rightleftharpoons Zn(OH)_3^- + 3H^+ \quad \log k = -28.4 \tag{3}$$

$$Zn^{2+} + 4H_2O \rightleftharpoons Zn(OH)_4^{2-} + 4H^+ \quad \log k = -41.2 \tag{4}$$

$$Zn(OH)_2(c) + 2H^+ \rightleftharpoons Zn^{2+} + 2H_2O \quad \log k = 11.5 \tag{5}$$

where k is the reaction equilibrium constant at 25 °C.

Considering the probable Zn transport in the layers of the study zone and influence on the sedimentary layers by the reclaimed layers, the initial $Zn(OH)_2(c)$ concentration of ②$_3$ and ④ was set as Zn concentration of sample Hg01-20 and Hg01-25 respectively, since no reclaimed layers covered their location (Fig. 1f). And initial $Zn(OH)_2(c)$ concentration of the dredge fills was set using the median of the detected Zn concentration in the neighboring ②$_3$ (Considering sample Hg04-16, Hg04-23, Hg05-21 in Fig. 1f). The initial Zn^{2+} concentration

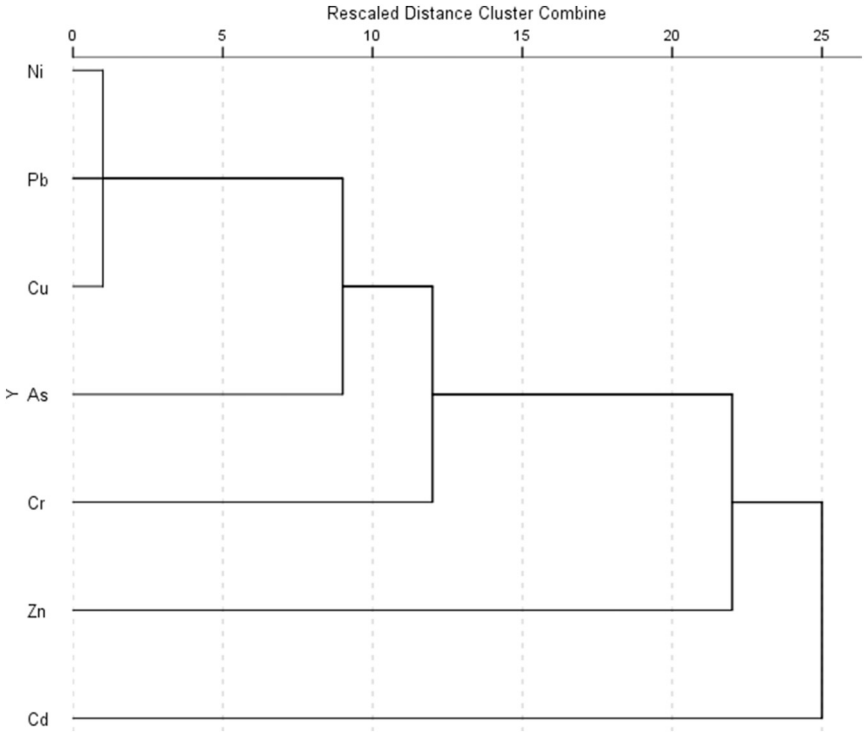

Fig. 5. Dendrogram of HCA showing the relevant association among Pb, Zn, Ni, Cu, Cr, Cd and As contents within sedimentary soils.

Table 5
Initial geotechnical and chemical parameters set in the numerical model.

	①$_{3-2}$			②$_3$	④	River
	Upper homogeneous fill	Clayey soil	Silty-sandy soil			
$Zn(OH)_2(c)$ (mol/L)	2.61×10^{-3}	2.61×10^{-3}	2.61×10^{-3}	7.12×10^{-4}	1.45×10^{-3}	
Zn^{2+} (mol/L)	9.91×10^{-9}	9.91×10^{-9}	9.91×10^{-9}	9.91×10^{-9}	9.91×10^{-9}	9.91×10^{-9}
pH	7.8	7.8	7.8	7.8	7.8	7.8
Pe	5.0	5.0	5.0	5.0	5.0	5.0
Porosity	0.50	0.51	0.43	0.45	0.58	
K_h (m/d)	3.92×10^{-1}	5.70×10^{-3}	3.92×10^{-1}	2.34×10^{-1}	5.16×10^{-4}	
K_v (m/d)	2.39×10^{-1}	4.13×10^{-3}	2.39×10^{-1}	1.62×10^{-1}	3.91×10^{-4}	
Specific storage (1/m)	0.0158	0.07899	0.0158	6.067E-03	0.06076	
Specific yield	0.28	0.05	0.28	0.21	0.02	

in the seepage was calculated considering chemical equilibrium (1–5), and no Zn was assumed in the precipitation. The temperature condition was set as 25 °C. The modeling term started from June 1st 2012 when the field was just reclaimed, the end time was November 30th 2016 when the specimen were sampled.

2.4.3. PHT3D model

PHT3D mode coupling PHREEQC-2 (Parkhurst and Appelo, 1999) with MT3DMS (Zheng and Wang, 1999) was introduced to simulate the transport of multi chemical components and changing pH (Prommer et al., 2003; Prommer and Post, 2010). The reactive transport equation for the nth (mobile) aqueous component is:

$$\frac{\partial C_n}{\partial t} = \frac{\partial}{\partial x_\alpha}\left(D_{\alpha\beta}\frac{\partial C_n}{\partial x_\beta}\right) - \frac{\partial}{\partial x_\alpha}(\upsilon_\alpha C_n) + \frac{q_s C_n^s}{\theta} + r_{reac,n} \quad (6)$$

and for immobile entities:

$$\frac{\partial C_n}{\partial t} = r_{reac,n} \quad (7)$$

where υ_α is the pore-water velocity in direction x_α (LT^{-1}), $D_{\alpha\beta}$ is the hydrodynamic dispersion coefficient tensor (L^2T^{-1}), q_s is a volumetric flow rate per unit volume of aquifer representing fluid sources (positive) and sinks (negative) (T^{-1}), θ is the porosity of the subsurface medium, C_n^s is the concentration of the source or sink flux (ML^{-3}), $r_{reac,n}$ is a source/sink rate due to chemical reaction ($ML^{-3}T^{-1}$) and C_n is the total aqueous component concentration of the nth component (ML^{-3}) (Yeh and Tripathi, 1989; Engesgaard and Kipp, 1992).

2.4.4. Drainage in the numerical model

Wide-spread drains with water table of 0.5–0.75 m deep were considered in the numerical model which facilitate draining of the field soils. The drainage channels in the numerical model result in unsaturated grids in large area (Fig. 2c). And the influence of the acid precipitation on the Zn transport within the field would not be effectively reflected. Thus to explore influence on Zn transport by acid precipitation in long term, only one typical drainage channel in the zone was considered in the numerical modeling, resulting in small-scale area of grids aborting during the modeling process and higher water head within the layers (Fig. 2d). Meanwhile, advection package, dispersion package and source/sink mixing package were applied in the PHT3D modeling.

Using the detected element concentrations within the deep soils and collected data, correlation analysis was performed among those data using PCA and HCA. Furthermore, assuming that ①$_{3-2}$ was Zn-polluted

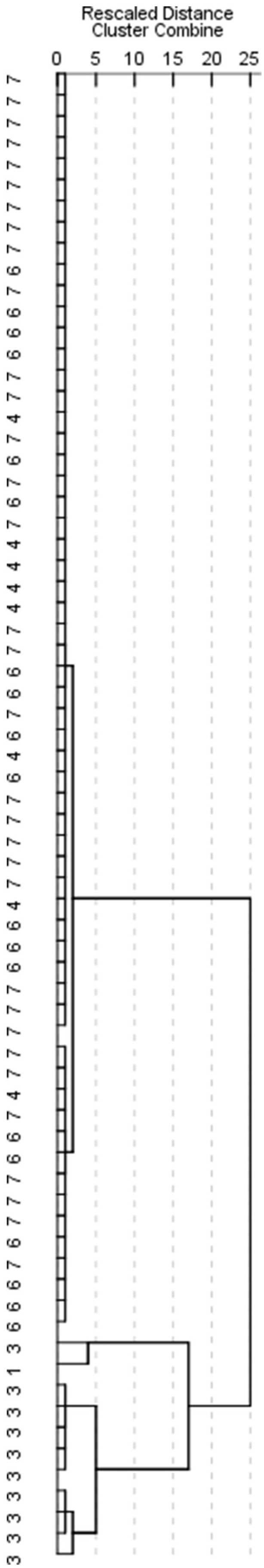

Fig. 6. Dendrogram of HCA showing correlation among different dredger fill types. 1 - muddy clay, 3 - silty clay, 4 - clayey silt, 6 - sandy silt, 7 - silty sand.

homogeneously, both ②$_3$ and ④ unpolluted when the modeled field was just reclaimed, Zn transport during 2012–2016 was modeled using the comprehensive geo-model and finite difference.

3. Results

3.1. Distribution of Zn contamination

Seven heavy metal elements including Zn, Cd, As, Ni, Cu, Pb and Cr were tested in laboratory. Only Zn exceeded the limit of level II in the surveyed zones. One dredger fill sample even exceeds the limit of level III. All the polluted specimens were sampled from the depth shallower than 38.5 m. Thus Zn was selected as the focused contaminant in this work.

Zn in specimens of ①$_{3-2}$, ①$_{3-3}$, ②$_3$, ④ and ⑤$_{1-1}$ exceeded the limit of level II. Sampling points of Zn over 300 ppm in Hengsha Island were detected in borehole Hg04–Hg07 (Fig. 1c, f). The Zn-contaminated dredger fills were found in the depth < 5 m. The concentration of Zn in shallow dredger fills (depth < 1 m) was remarkably lower than the deep ones (Figs. 3a and 4a). Contaminated points in Laogang Town were disclosed within stratum ①$_{3-3}$, ②$_3$, ④ and ⑤$_{1-1}$ (Fig. 1g, i), no dredger fill was detected over the limit of level II. And the previous drainage channel soil Lg04–04 in stratum ①$_{3-3}$ exceeded the limit of level II, significantly varied from its neighboring detected points (Fig. 4b). The two sampling points in borehole Yl01 also showed very low level of Zn. Zn concentration shows no explicit correlation with soil types (Fig. 1a–b). The concentration of Zn exceeding the limit of level II was detected in both clayey soils and silty- sandy soils in several points (Fig. 3b).

3.2. Potential origination of Zn

PCA on Zn, Mn and Fe of both dredger fills and sedimentary soils shows that the first two principal component (PCs) explained 97.59% of the total variance (i.e., PC1 and PC2 respectively explained 67.16% and 30.43% of the variance). PC1 had a strong positive relationship with Fe and Mn. PC2 had a highly positive relationship with Zn (Table 4). HCA shows that the association among Cd, Zn and the other five heavy metal elements was low (Fig. 5).

The parameters of the numerical model were determined on basis of the field survey, Detection using inductively coupled plasma optical emission spectrometer (ICP) and other geotechnical test materials (Table 5). HCA analysis on different dredger fill types shows that clayey fills are differed from silty and sandy fills significantly in the study zones (Fig. 6). The difference validates soil type division in the stochastic geo-model for heterogeneous reclaimed layers in the modeled field by Wang et al. (2019) (Fig. 2a). The distribution of $Zn(OH)_2$, Zn^{2+} and pH in the surface layer (depth of 0–0.4 m) changed significantly during the modeling term. $Zn(OH)_2$ in most area of the surface layer decreased from 2.61×10^{-3} mol/L (307.32 ppm) to 2.50×10^{-3}–2.53×10^{-3} mol/L, less than the limit of level II (2.55×10^{-3} mol/L) (Fig. 7a–b). $Zn(OH)_2$ decreased significantly in the second layer (depth of 0.4–0.8 m) mainly around the drainage channel (Fig. 7c). Significant decreasing of $Zn(OH)_2$ was figured out just within the upper three layers (Fig. 7d). $Zn(OH)_2$ did not significantly change in bottom layer of the dredger fill (depth of 11.2–11.6 m) (Fig. 7e). The concentration of $Zn(OH)_2$ within top layer of ②$_3$ was detected changing at four corners in small scale (Fig. 7f), and the change becomes less downward to the bottom of stratum ④.

Both Zn^{2+} and pH changed remarkably during the modeling term, and their distribution in dredger fills no deeper than 4.8 m was explicitly controlled by drainage channel and water head (Fig. 8). The pH

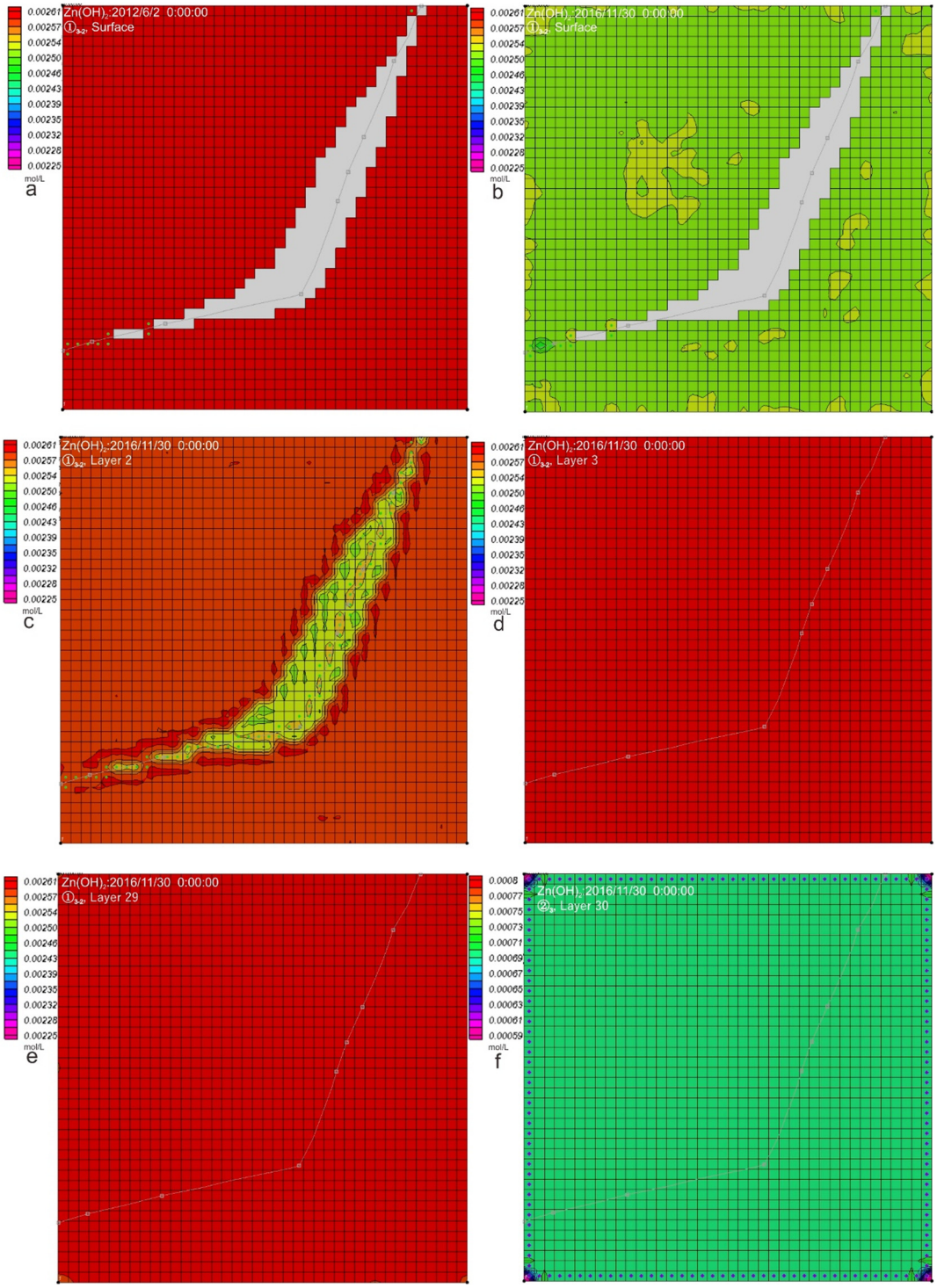

Fig. 7. $Zn(OH)_2$ concentration distribution within layers. a. Initial $Zn(OH)_2$ concentration distribution within surface on June 2nd 2012; b. $Zn(OH)_2$ concentration distribution within surface on November 30th 2016; c. $Zn(OH)_2$ concentration distribution within depth of 0.4–0.8 m on November 30th 2016; d. $Zn(OH)_2$ concentration distribution within layer 4 (depth of 1.2–1.6 m) on November 30th 2016; e. $Zn(OH)_2$ concentration distribution within bottom of heterogeneous fill (depth of 11.2–11.6 m) on November 30th 2016; f. $Zn(OH)_2$ concentration distribution within top of stratum ②$_3$ on November 30th 2016.

ranged from 8.41 to 8.44 in large belt around the drainage channel in depth of 0.4–0.8 m, slightly higher than the detected 7.7–8.2 in field surveys. Meanwhile, Zn^{2+} ranged from 8×10^{-6} mol/L to 1×10^{-5} mol/L, slight higher than the detected 3×10^{-7}–6×10^{-7} mol/L in the modeled zone. Heterogeneous distribution of Zn^{2+} and pH within layer 13 (Fig. 8e–f) correlates with soil heterogeneity within it (Fig. 8c), higher Zn^{2+} concentration and lower pH can be detected in silty-sandy soils than neighboring clayey soil.

The decreasing rate of $Zn(OH)_2$ from the top layer of the homogeneous dredger fill (0–0.4 m) to the top layer of the heterogeneous dredger fills (2.0–2.4 m) declined sharply. The rate during rainstorms was remarkably higher than that during the remaining constant precipitation periods. The rate of the drainage points was higher than that of the points far from the drainage and the model boundaries. $Zn(OH)_2$-reduction in monitored points of layer 6 (2.0–2.4 m), bottom layer of the dredger fills (11.2–11.6 m) and top layer of ②$_3$ (11.6–14.1 m) during

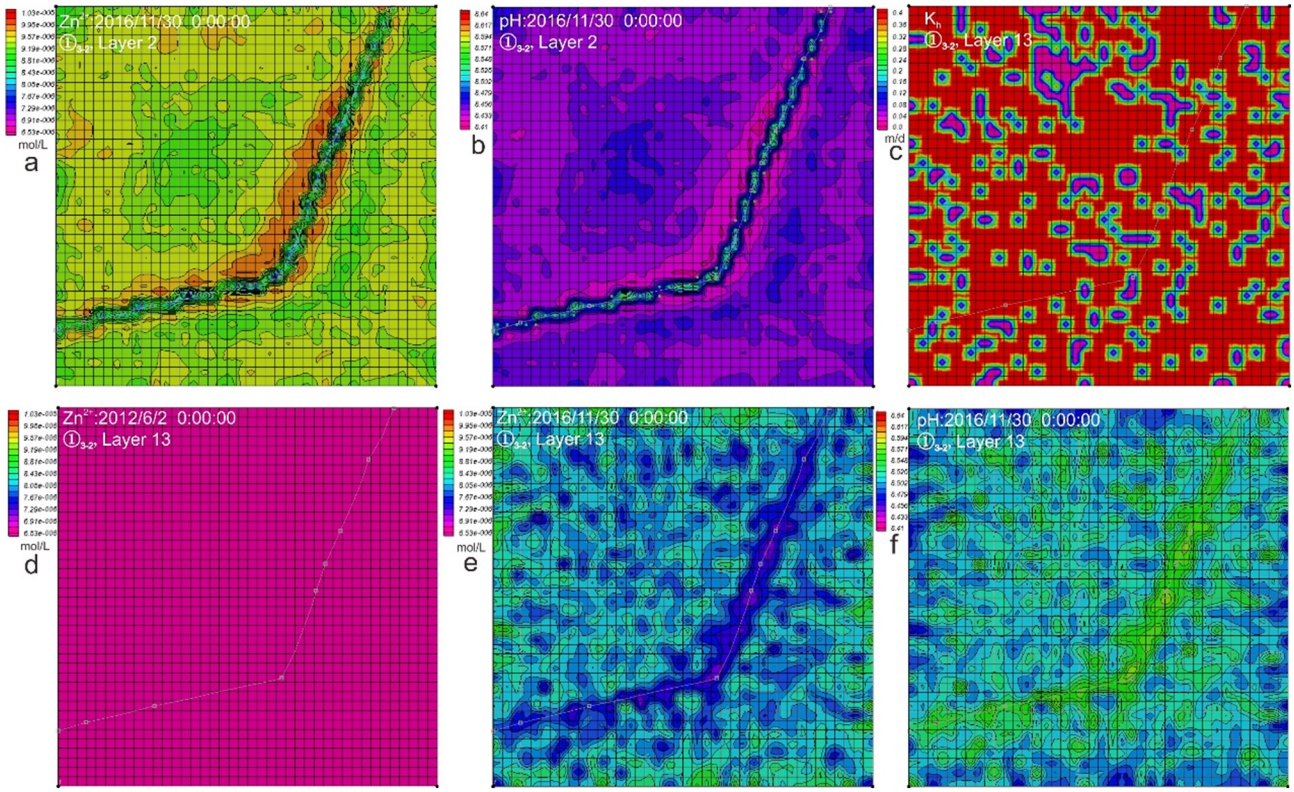

Fig. 8. Zn^{2+}, pH, K_h contour distribution in the geo-model. a. Zn^{2+} concentration distribution within depth of 0.4–0.8 m on November 30th 2016; b. pH distribution within layer 2 on November 30th 2016; c. K_h contour distribution within of heterogeneous fill (layer 13, depth of 4.8–5.2 m); d. Initial Zn^{2+} concentration distribution within layer 13 on June 2nd 2012; e. Zn^{2+} concentration distribution within layer 13 on November 30th 2016; f. pH distribution within layer 13 on November 30th 2016.

the modeling term all turns out $< 5 \times 10^{-6}$ mol/L (Fig. 9a). Zn^{2+} concentration in these monitored points evolved in an opposite trend of pH. The total change of both Zn^{2+} concentration and pH in the upper two layers of dredger fills and layer 6 was remarkably higher than those in depth of 11.2–14.1 m (layer 29–30) (Fig. 9b–c). Both Zn^{2+} concentration and pH of points within the three layers response intensively to rainstorms, which does not happen in layer 29–30. Thus, monitored points in the upper two layers of dredger fills and layer 6 were divided into strong response segment, and points in depth of 11.2–14.1 m were divided into weak response segment (Fig. 9d). In the strong response segment, the influence of rainstorms on Zn^{2+} was similar to that of pH, higher in interior soil points of the upper two layers of dredger fills, and clayey points of layer 6, rainstorm contribution ratio in block points of the upper two layers of dredger fills and clayey points of layer 6 shows larger than 100%. The contribution of rainstorm to $Zn(OH)_2$ -decrease in two points of the surface layer both shows around 34%, and 43%, 66% respectively in block point and drainage point of the second layer of homogeneous dredged fil. The influence trend on $Zn(OH)_2$ in layer 6 was similar to that of both Zn^{2+} concentration and pH. Besides, the influence on change of both Zn^{2+} concentration and pH within the top layer and interior points of layer 2 by the two rainstorms per year becomes less and less during the modeling period. Rainstorm contribution to change of three chemical components in the weak response segment all shows < 10% (Fig. 9d).

4. Discussion

4.1. Disclosure of Zn contamination

The previous works did not report Zn contamination within shallow dredger fills (depth < 1 m) of Hengsha Island and Laogang Town (Wang et al., 2018). Further work based on three batches of ICP detection disclosed that Zn contamination (Zn over 300 ppm) did exist within some parts of the deep reclaimed layers, ②$_3$, ④ and ⑤$_{1-1}$. Deep soils in large area contained Zn exceeding the limit of level II, even over the limit of level III, thus potential risk for both nowadays ecosystem and future development existed herein.

4.2. Zn origination

PCA indicated that Zn in these soils held a different major source from that of Fe and Mn. The Zn contamination was artificially added to the soils, because major elements, Fe and Mn, are usually viewed as deposited into soils during sedimentary process (Martin et al., 2006; Mico et al., 2006). HCA implied that the source of Zn in the sedimentary soils is different from that of Cd and group of As, Ni, Cu, Pb and Cr, which is different from HCA on the seven heavy metal elements in the surface dredger fills by Wang et al. (2018). This was probably caused by the different transport processes among these elements during the land reclamation construction and the long term effects by exterior factors such as acid precipitation, plant uptake.

Soil type in many contaminated points belonged to clayey soils in ④ and ⑤$_{1-1}$, and showed no identifiable impact on Zn concentration within the reclaimed layers. Thus soil heterogeneity in dredger fills held no significant correlation with its initial Zn concentration. Large-scale Zn-contamination exists under both the dredger fill layers and other surface layers, implying that the Zn contamination was not caused by the hydraulic land reclamation or the dredger fills. Numerical modeling also showed that no significant Zn transport from the contaminated dredger fill layers to the underlying sedimentary layers. No Zn contamination was detected in borehole Hg01 or Yl01. Thus the detected Zn contamination in stratum ②$_3$, ④ and ⑤$_{1-1}$ was not formed during their deposition processes, which can also be verified by both the HCA and PCA results. Seldom artificial exploitation was conducted in

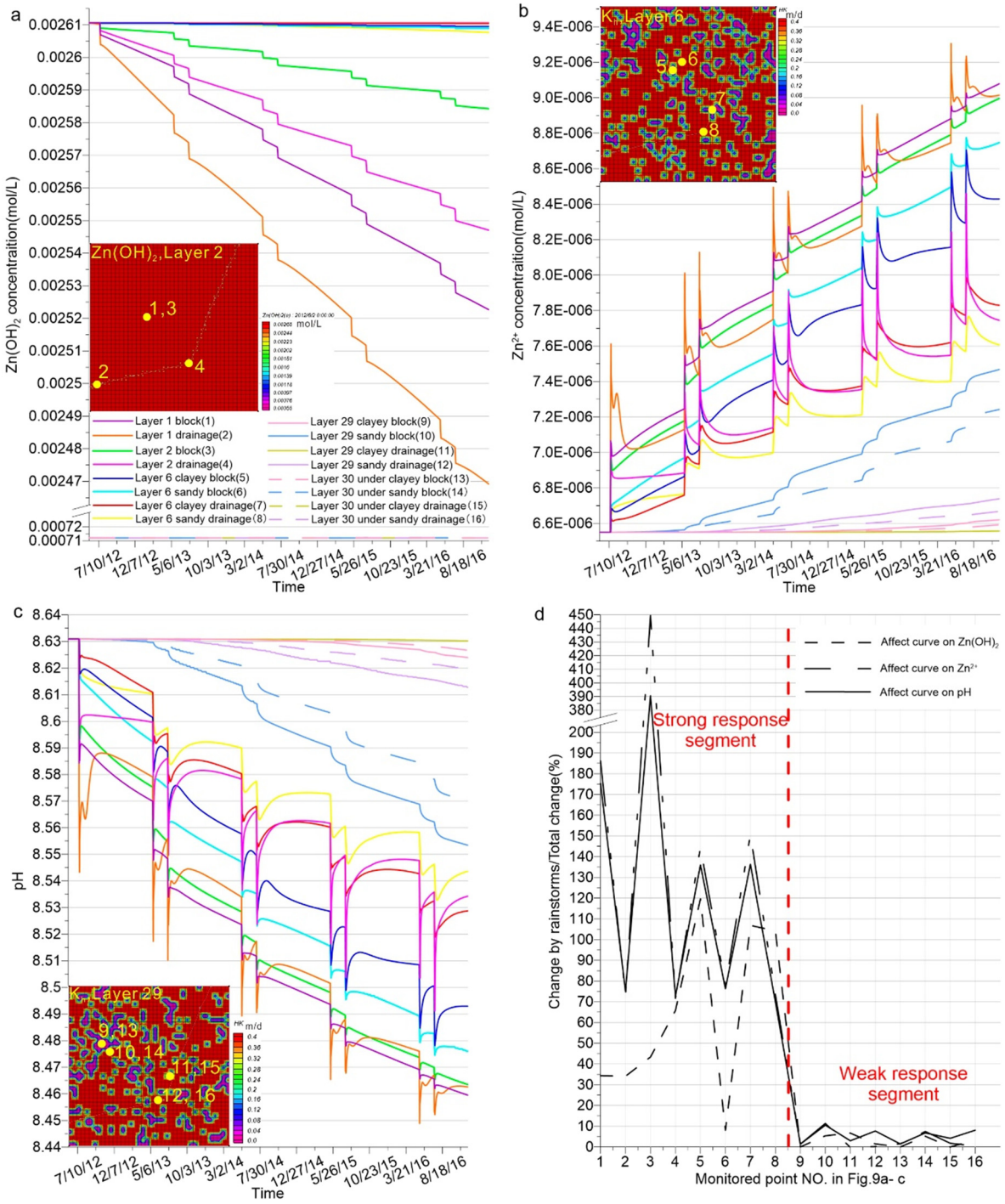

Fig. 9. Solute transport within single grids of the numerical model. a. $Zn(OH)_2$ concentration evolution; b. Zn^{2+} concentration evolution; c. PH concentration evolution; d. Rainstorm contribution on solute transport during the analyzed period.

reclaimed land of Hengsha Island, meaning that the deep contamination Zn in the reclaimed layers was not formed after the land was reclaimed in 2012. The Zn contamination within the deep reclaimed soils was originated from fill source such as stratum ②$_3$, ④ in the neighboring waters. The high level of Zn in the previous drainage soil sample Lg04-04 implied that one major contamination source of the Zn contamination within sediments in the neighboring waters was discharge of sewage by factories in neighboring coastal zones. Considering flushing by precipitation and draining by amounts of channels in the reclaimed areas, the widespread low level Zn in the surface dredger fills of Hengsha Island can be explained, although their fill source probably was also Zn-contaminated heterogeneously like the deep reclaimed fills, which can be reflected by the no significant $Zn(OH)_2$-change from 2012 to 2016 in the numerical modeling.

The simulated Zn contamination mainly in formulate of $Zn(OH)_2$ in November 2016 was significantly higher than the detected Zn within surface layer of dredger fills, resulting directly in the pH higher than the detected ones. Several reasons probably contributed to the result. Firstly, different from initially homogeneous Zn-contamination in the model, Zn concentration exceeded the limits existed only in some parts of the field (Fig. 4a), which probably decelerates the depollution of Zn in the numerical analysis. Secondly, only one drainage channel was

modeled to enable most part of the surface layer keep saturated during the modeling process (Fig. 2c–d), but amounts of drainage channels exist in the field (Fig. 1d, h), thus the quick decrease of $Zn(OH)_2$ concentration by multi-channels was not characterized in the numerical modeling. Thirdly, bushy phragmite and typha grow in the reclaimed zones (Fig. 1e), actually, these plants can absorb much heavy metal elements including Zn from the soils (Duman et al., 2015; Kumari and Tripathi, 2015). Besides, much surface run-off was produced during rainstorm stages since the infiltration cannot enable all the precipitation by rainstorms to enter the layers, soil flushing process by the surface ruff-off was not included in the numerical model, and this probably weakens Zn remediation by the acid precipitation.

4.3. Countermeasures

Soil contamination within saturated belt is required to be monitored as unsaturated soils in Shanghai (SMBEE, 2016b). The detected Zn contamination in the study zones remains to be depolluted. Considering the depth of the Zn contamination was deeper than 5 m, field remediation methods treating deep soil contaminations were probably effective herein. Though rainstorms held key impacts on Zn-depollution within the deep dredger fills in the numerical modeling, it depends on the weather and needs too long time. In-situ water flushing (Mao et al., 2015) using eluents heightening Zn-transportability within the soils such as acid, Ammonium-based deep eutectic solvents (Mukhopadhyay et al., 2016), and permeable reactive barriers (Obiri-Nyarko et al., 2014) all were proved efficient for removing deep Zn contamination. Though ex-situ soil washing can also remediate soil Zn contamination (Feng et al., 2001), but it would take a great cost for so large-scale deep contaminated zones herein. Besides, electro-kinetic remediation (Pazos et al., 2006) probably can be effective for the deep Zn contamination. Dredger fill layers in the study zones are still unconsolidated, which means porosity within them is still higher, thus field remediation for the deep Zn contamination should be conducted as soon as possible so that the high soil porosity can be taken advantage.

5. Conclusions

With Shanghai's newly reclaimed fields as a typical background, field survey, lab detection and numerical modeling results in this work showed that:

(1) Zn contamination heterogeneously exists within saturated belt deeper than 1.8 m in both reclaimed zones of Hengsha Island and Laogang Town in Shanghai. The contaminated layers include deep dredger fill layers ($①_{3-2}$), $①_{3-3}$, $②_3$, ④ and $⑤_{1-1}$ in the surveyed zones. No heavy metal element of Cd, As, Ni, Cu, Pb and Cr was detected to be over limits within these layers, and the strata $⑤_{1-2}$ to ⑨ showed good soil environment quality.
(2) The Zn contamination within the deep sediments was formed due to exogenous contamination source before the land reclamation construction, and the slight alkali environment in the reclaimed regions resulted in weak Zn transport between the dredger fills and the underlying sedimentary layers. The Zn contamination within the deep dredger fills was probably from the fill source, and initially held no correlation with soil type of the fills. But heterogeneity of dredger fills could differentiate Zn-depollution rate within the reclaimed layers.
(3) Flushing process by acid precipitation and draining process due to widespread drainage channels in the reclaimed zones contributed much to the depollution of the Zn contamination shallower than 1.2 m. Rainstorms remarkably facilitated Zn reduction below 0.4 m since the fields were reclaimed.
(4) PH-control and electro-kinetic remediation can be considered as remediation measures for the deep Zn contamination within alkali reclaimed land. Un-consolidation state of the dredger fills can be used to facilitate the remediation process.

Acknowledgements

This work is sponsored by National Key Research and Development Program of China, China (2017YFC0806000), Shanghai Municipal Science and Technology Commission, China project (18DZ1201301), SKLGP Opening fund of (SKLGP2018K019), of State Key Laboratory of Geohazard Prevention and Geoenvironmental Protection (Chengdu University of Technology), China Key Laboratory of Karst Collapse Prevention; CAGS, China and IGCP, UNESCO Project (663-La Subsidence in Coastal cities).

References

Appelo, C.A.J., Rolle, M., 2010. PHT3D: a reactive multicomponent transport model for saturated porous media. Ground Water 48 (5), 627–632.
Bekhit, H.M., Hassan, A.E., 2005. Two-dimensional modeling of contaminant transport in porous media in the presence of colloids. Adv. Water Resour. 28 (12), 1320–1335.
Caeiro, S., Costa, M.H., Ramos, T.B., Fernandes, F., Silveira, N., Coimbra, A., 2005. Assessing heavy metal contamination in Sado Estuary sediment: an index analysis approach. Ecol. Indic. 5 (2), 151–169.
Carle, S.F., 1999. T-PROGS: Transition Probability Geostatistical Software Version 2.1. Hydrologic Sciences Graduate Group University of California, Davis.
Carle, S.F., Fogg, G.E., 1997. Modeling spatial variability with one and multidimensional continuous lag Markov chains. Math. Geol. 29 (7), 891–918.
CEPB — China's Environmental Protection Bureau, CTSB — China's Technical Supervision Bureau, 1995. Environmental quality standards for soil. Available online on. http://kjs.mep.gov.cn/hjbhbz/bzwb/trhj/trhjzlbz/199603/t19960301_82028.htm.
Duman, F., Urey, E., Koca, F.D., 2015. Temporal variation of heavy metal accumulation and translocation characteristics of narrow-leaved cattail (Typha angustifolia L.). Environ. Sci. Pollut. Res. 22 (22), 17886–17896.
Engesgaard, P., Kipp, K.L., 1992. A geochemical transport model for redoxcontrolled movement of mineral fronts in groundwater flow systems: a case of nitrate removal by oxidation of pyrite. Water Resour. Res. 28 (10), 2829–2843.
EPA—United States Environmenal Protection Agency, 1989. Characteristics and effects of dredged material disposal in the marine environment. Available online on. https://nepis.epa.gov/Exe/ZyNET.exe/9101PADQ.TXT?ZyActionD=ZyD.
EPA—United States Environmental Protection Agency, 2016. Assessment of contaminated sediments in the Kinnickinnic River Mooring Basin in the Milwaukee Estuary Area of Concern, Milwaukee, Wisconsin. Available online on. https://dnr.wi.gov/topic/greatlakes/documents/TurningBasinSiteCharacterizationReport.pdf.
Erftemeijer, P.L.A., Riegl, B., Hoeksema, B.W., Todd, P.A., 2012. Environmental impacts of dredging and other sediment disturbances on corals: a review. Mar. Pollut. Bull. 64 (9), 1737–1765.
Fang, M., Wu, Y.J., Liu, H., Jia, Y., Zhang, Y., Wang, X.T., Wu, M.H., Zhang, C.L., 2013. Distribution, sources and ecological risk assessment of heavy metals in sediments of the Yangtze River estuary. Acta Sci. Circumst. 33 (2), 563–569.
Feng, D., Lorenzen, L., Aldrich, C., Mare, P.W., 2001. Ex situ diesel contaminated soil washing with mechanical methods. Miner. Eng. 14 (9), 1093–1100.
Gotelli, N.J., Ellison, A.M., 2004. A Primer of Ecological Statistics, 1st ed. 492 Sinauer Associates, Sunderland, MA, USA.
Ho, K.T., Burgess, R.M., Pelletier, M.C., Serbst, J.R., Ryba, S.A., Cantwell, M.G., 2002. An overview of toxicant identification in sediments and dredged materials. Mar. Pollut. Bull. 44 (4), 286–293.
Kedziorek, M.A.M., Dupuy, A., Bourg, A.C.M., Compère, F., 1998. Leaching of Cd and Pb from a polluted soil during the percolation of EDTA: laboratory column experiments modeled with a non-equilibrium solubilization step. Environ. Sci. Technol. 32 (11), 1609–1614.
Kumari, M., Tripathi, B.D., 2015. Efficiency of Phragmites australis and Typha latifolia for heavy metal removal from wastewater. Ecotoxicol. Environ. Saf. 112, 80–86.
Li, L., Ping, X.Y., Wang, Y.L., Jiang, M., Yuan, Q., Shen, X.Q., 2013. Study on the spatial and temporal distribution of the heavy metals in the surface sediments based on multivariate statistical technique from the Changjiang Estuary and its adjacent areas. Environ. Chem. 32 (3), 438–445.
Liu, L., Xu, S.Y., Chen, Z.L., Yu, J., 2000. Spatial distribution and environmental quality assessment on heavy metals in tidal flat sediments of Shanghai coastal zone. Shanghai Geol. 1, 1–5.
Lu, M., Liu, M., Hou, L.J., Ou, D.N., Quan, R.S., Xu, S.Y., Yu, L.Z., 2010. Characteristic of rainfall in Shanghai and its influence on urban flood disaster. J. Nat. Dis. 19 (3), 7–12.
Mallants, D., Van Genuchten, M.T., Šimůnek, J., Jacques, D., Seetharam, S., 2011. Leaching of contaminants to groundwater. In: Swartjes, F. (Ed.), Dealing with Contaminated Sites. Springer, Dordrecht, pp. 828–839.
Manap, N., Voulvoulis, N., 2016. Data analysis for environmental impact of dredging. J. Clean. Prod. 137, 394–404.
Mao, X., Jiang, R., Xiao, W., Yu, J., 2015. Use of surfactants for the remediation of contaminated soils: a review. J. Hazard. Mater. 285, 419–435.
Martin, J.A.R., Arias, M.L., Corbi, J.M.G., 2006. Heavy metal contents in agricultural top soils in the Ebro basin (Spain). Application of the multivariate geo-statistical methods to study spatial variations. Environ. Pollut. 144, 1001–1012.

Martín-Antón, M., Negro, V., del Campo, J.M., López-Gutiérrez, J.S., Esteban, M.D., 2016. Review of coastal land reclamation situation in the world. J. Coast. Res. 75 (sp1), 667–671.
Mico, C., Recatala, L., Peris, M., Sanchez, J., 2006. Assessing heavy metal sources in agricultural soils of an European Mediterranean area by multivariate analysis. Chemosphere 65, 863–872.
Morbidelli, R., Corradini, C., Saltalippi, C., Flammini, A., Dari, J., Govindaraju, R.S., 2018. Rainfall infiltration modeling: a review. Water 10, 1873–1893.
Mostafa, Y.E.S., 2012. Environmental impacts of dredging and land reclamation at Abu Qir Bay, Egypt. Ain Shams Eng. J. 3 (1), 1–15.
Mukesh, M.V., Chandrasekaran, A., Premkumar, R., Keerthi, B.N., 2018. Metal enrichment and contamination in river and estuary sediments of Tamirabarani, South India. J. Earth Sci. Clim. Chang. 9 (10), 497–503.
Mukhopadhyay, S., Mukherjee, S., Adnan, N.F., Hayyan, A., Hayyan, M., Hashim, M.A., Gupta, B.S., 2016. Ammonium-based deep eutectic solvents as novel soil washing agent for lead removal. Chem. Eng. J. 294, 316–322.
Nezhad, M.M., Javadi, A.A., Rezania, M., 2011. Modeling of contaminant transport in soils considering the effects of micro- and macro-heterogeneity. J. Hydrol. 404 (3–4), 332–338.
Nützmann, G., Viotti, P., Aagaard, P., 2005. Reactive Transport in Soil and Groundwater. Springer, Berlin Heidelberg.
Obiri-Nyarko, F., Grajales-Mesa, S.J., Malina, G., 2014. An overview of permeable reactive barriers for in situ sustainable groundwater remediation. Chemosphere 111, 243–259.
Parkhurst, D.L., Appelo, C.A.J., 1999. User's guide to PHREEQC (V. 2) —a computer program for speciation, batch-reaction, one-dimensional transport, and inverse geochemical calculations. In: USGS Water-Resources Investigations Report 99–4259. US Geological Survey, Denver, Colorado.
Pazos, M., Sanromán, M.A., Cameselle, C., 2006. Improvement in electrokinetic remediation of heavy metal spiked kaolin with the polarity exchange technique. Chemosphere 62 (5), 0–822.
Prommer, H., Post, V., 2010. PHT3D: a reactive multicomponent transport model for saturated porous media (V. 2.10), user's manual. Available online on. http://www.pht3d.org.
Prommer, H., Barry, D.A., Zheng, C.M., 2003. MODFLOW/MT3DMS-based reactive multi component transport modeling. Ground Water 41 (2), 247–257.
Reichle, R.A., Mccurdy, K.G., Hepler, L.G., 1975. Zinc hydroxide: solubility product and hy-droxy-complex stability const. Can. J. Chem. 53 (24), 3841–3845.
SMBEE—Shanghai Municipal Bureau of Ecology and Environment, 2013. Shanghai environmental bulletin in 2012. Available online on. http://www.sepb.gov.cn/fa/cms/shhj/file/2013bulletin/index.html.
SMBEE—Shanghai Municipal Bureau of Ecology and Environment, 2014. Shanghai environmental bulletin in 2013. Available online on. http://www.sepb.gov.cn/fa/cms/shhj//shhj2143/shhj2144/2014/06/86642.htm.
SMBEE—Shanghai Municipal Bureau of Ecology and Environment, 2015. Shanghai environmental bulletin in 2014. Available online on. http://www.sepb.gov.cn/fa/cms/shhj//shhj2143/shhj2144/2015/06/89703.htm.
SMBEE—Shanghai Municipal Bureau of Ecology and Environment, 2016a. Shanghai environmental bulletin in 2015. Available online on. http://www.sepb.gov.cn/fa/cms/shhj//shhj2143/shhj2144/2016/03/92097.htm.
SMBEE—Shanghai Municipal Bureau of Ecology and Environment, 2016b. Shanghai technical guidelines for environmental site monitoring. Available online on. http://www.sepb.gov.cn/fa/cms/upload/uploadFiles/2016-09-13/file2459.pdf.
SMBEE—Shanghai Municipal Bureau of Ecology and Environment, 2017. Shanghai environmental bulletin in 2016. Available online on. http://www.sepb.gov.cn/fa/cms/shhj//shhj2143/shhj2144/2017/06/96217.htm.
Stark, T.D., Choi, H., Schroeder, P.R., 2005. Settlement of dredged and contaminated material placement areas. II: primary consolidation, secondary compression, and desiccation of dredger fill input parameters. J. Waterw. Port Coast. Ocean Eng. 131 (2), 52–61.
Sun, L., Jia, T., Zhuo, R., Yan, S., Guo, B., 2015. Numerical solutions for consolidation of under-consolidated dredger fill under vacuum preloading. In: Mi, W., Lee, L.H., Hirasawa, K., Li, W. (Eds.), Recent Developments on Port and Ocean Engineering. Journal of Coastal Research, Special Issue, No. 73pp. 277–282 Coconut Creek (Florida), ISSN 0749-0208.
Sun, X.S., Fan, D.J., Liu, P.F., Pang, Y., Tian, Y., 2017. The states of Eh, pH of water from Yangtze River estuary and its adjacent areas and their implications. Adv. Mar. Sci. 35 (1), 96–106.
UN Altas, 2019. Coasts and coral reefs. Available online on. http://www.oceansatlas.org/subtopic/en/c/304/.
Wang, W., Liu, H., Li, Y., Su, J., 2014. Development and management of land reclamation in China. Ocean Coast. Manag. 102, 415–425.
Wang, J.X., Wu, L.B., Deng, Y.S., Song, D.S., Liu, W.J., Hu, M.Z., Liu, X.T., Zhou, J., 2018. Investigation and evaluation of contamination in dredged reclaimed land in China. Mar. Georesour. Geotechnol. 36 (5), 603–616.
Wang, J.X., Wu, L.B., Yan, X.X., Wu, Z., Long, G.H., Wang, H.M., Xu, N., 2019. Clean Hydraulic Reclamation Technology and Clean Foundation Treatment Technology -Countermeasures to Contaminated Fills. EGRWSE-2019, Chicago, United States, pp. 166–170 (In Press).
Yang, K., Tang, M., Zhou, L.Y., 2004. Variation of evaporation and evaporation differences between proper and suburb in Shanghai in recent 30 years. Sci. Geogr. Sin. 24 (5), 557–561.
Yeh, G.T., Tripathi, V.S., 1989. A critical evaluation of recent developments in hydrogeochemical transport models of reactive multi chemical components. Water Resour. Res. 25 (1), 93–108.
Zhang, W., Feng, H., Chang, J., Qu, J., Xie, H., Yu, L., 2009. Heavy metal contamination in surface sediments of Yangtze River intertidal zone: an assessment from different indexes. Environ. Pollut. 157 (5), 1533–1543.
Zheng, C.M., Wang, P.P., 1999. MT3DMS: A Modular Three Dimensional Multispecies Transport Model for Simulation of Advection, Dispersion, and Chemical Reactions of Contaminants in Groundwater Systems. Documentation and User's Guide. US Army Corps of Engineers, Washington, DC.